Eur. Phys. J. B **83**, 173–179 (2011)
DOI: 10.1140/epjb/e2011-20253-4

THE EUROPEAN PHYSICAL JOURNAL B

Regular Article

Transport properties of orbitally hybridized organic semiconductors

S.J. Sun[1,2,a], C.Y. Lin[2], and C.F. Yu[3]

[1] Department of Applied Physics, National University of Kaohsiung, 811 Kaohsiung, Taiwan, R.O.C.
[2] Department of Physics, National Chung Hsing University, 402 Taichung, Taiwan, R.O.C.
[3] Department of Applied Physics, National Chiayi University, 600 Chiayi, Taiwan, R.O.C.

Received 30 March 2011 / Received in final form 7 August 2011
Published online 23 September 2011 –

Abstract. A microscopic theory based on the orbital hybridization model via single orbital approximation is developed to calculate the current variation in organic semiconductors that are coupled to the external orbits from the environment. The charge transfer resulted from the orbital hybridization between the environment and the organic semiconductor rebuilds the energy levels and eventually alters the transport properties of the organic semiconductor. Two parameters in our theory, the orbital energy level of the environment relative to the energy level of organic semiconductor and the orbital hybridization interaction, dominate the current variation in the organic semiconductors. Our results show that the suppression of atomic dimerization due to orbital hybridization gives rise to an increase of electrical conduction in organic semiconductor. Also, after coupling with the environment, the charge-donating organic semiconductors are more conductive than the charge-accepting ones.

1 Introduction

Organic semiconductors (OSCs) are gradually attracting researchers' attentions not only owing to their interesting physical properties but also to their great potential in future applications to molecular devices [1–3]. Thus it is necessary to investigate the charge transport properties of the material before it is employed for devices applications [4–7]. Generally speaking, except for those shielded with insulating coatings, all materials are bound to be influenced by the environment. Therefore, for most cases it is necessary to construct theories with the effects of environment encorporated. Since the molecular weight of OSC is lighter than that of inorganic semiconductors (IOSC), therefore, compared with IOSC, OSC is more sensitive to the external couplings from the environment. External couplings to OSC has been studied [8] and considered in the device application such as the gas sensors [9–11]. In fact, external couplings occur in any hybri-OSC system, for instance, once OSC is deposited on a substance or itself adsorbs enough gases molecules (which we hereafter refer to as the "environment" (ENV)) to form hybri-junctions, the hybridization of the electronic orbitals of the substance or the ENV hybridize with that of the OSC will lead to a redistribution of charges, which is named as the charge transfer (CT) between the OSC and the ENV [12,13].

CT is obviously a physical process of great importance in bonding formation and transport properties among atoms and molecules. Other than the orbital hybridization, CT can also be induced through other mechanisms, for instance, electron-phonon (e-ph) interactions, which evidently exists strongly in OSC and form polarons through carriers in OSC [14]. Besides, the essential mechanical property of OSC, the electrical field screening inside OSC, and the energy level difference between the orbits of OSC and ENV [15–17] can also be sources of producing CT. In addition, Coulomb barrier established in the interface of the hybri-OSC is another factor to produce CT [18,19].

For the simplicity, we select a quasi-one dimensional OSC as the sample, i.e., acetylene like OSC [20], which has been extensively studied by Su-Schrieffer-Heeger (SSH) model [21,22]. Via single orbital approximation we establish a formula to simulate the CT process between the OSC and the ENV and calculate the current in the OSC under various couplings to the ENV by employing Keldysh non-equilibrium Green's function method. The theory developed here is applicable to simulate CT process in DNA, which is strongly coupled with ENV molecules [23].

The paper is organized as follows. Section 2 is the theoretical description, in which we demonstrate our theoretical model and the methods used in detail. In Section 3, we exhibit our results and discussions. Finally, there is a summary in the end.

2 Theoretical description

The total Hamiltonian of our model consists of three subsystems,

$$H = H_e + H_s + H_E. \tag{1}$$

[a] e-mail: sjs@nuk.edu.tw

H_e, represented in the semi-classical form, is the electronic part of Hamiltonian in the traditional SSH model with the strong electron-phonon (e-ph) coupling existing in the OSC system,

$$H_e = \sum_{n,\sigma} \epsilon_0 |c_{n,\sigma}\rangle\langle c_{n,\sigma}| - \sum_{n,\sigma} t_{n,n+1}(|c_{n+1,\sigma}\rangle\langle c_{n,\sigma}| + h.c.) + \frac{K_s}{2}\sum_n (u_{n+1} - u_n + C)^2, \quad (2)$$

where $t_{n,n+1} = t_0 - \alpha(u_{n+1} - u_n) + (-)^n t_e$ and ϵ_0 is the orbital energy level in the nth site state $|c_{n,\sigma}\rangle$ of OSC with spin index σ; t_0 is the hopping integral in the OSC; u_n is the atomic displacement for the nth molecule, and α is the e-ph coupling constant; t_e is a small energy for diminishing the energy degeneracy. The last term represents the spring potential with an effective spring constant K_s, and the constant C is determined by the length conservation.

When the bias V_a is applied to the OSC and if the electric field is not screened completely, the electrical energy H_E arises,

$$H_E = \sum_{n,\sigma} V(n)(|c_{n,\sigma}\rangle\langle c_{n,\sigma}| - 1), \quad (3)$$

where $V(n)$ is the electrical potential energy on nth molecular site. In the linear potential drop approximation the constant electric field, $E = \frac{V_a}{(N-1)a}$ and $V(n) = -e[V_a - E((n-1)a + u_n]$, where N and a are the total molecular sites and the bond length of the OSC, respectively. However, if the electrical field is screened completely, i.e. $E = 0$ then $V(n) = 0$.

H_s in the Hamiltonian is the orbital coupling between the OSC and the ENV,

$$H_s = V\left(\sum_{n,\sigma} |c_{n,\sigma}\rangle\langle d_{n,\sigma}| + h.c.\right) + E_p \sum_{n,\sigma} |d_{n,\sigma}\rangle\langle d_{n,\sigma}|, \quad (4)$$

where the first term represents the orbital hybridization between the orbits of the OSC and the ENV via the coupling constant V, and the second term represents the on-site term with E_p denoting the orbital energy level of ENV.

The bases $|c_{n,\sigma}\rangle$ and $|d_{n,\sigma}\rangle$ in equation (1) represent the states for the OSC and the ENV in the nth molecular site, respectively, and both states are not necessarily orthogonal to each other. Herein, we construct a new bases set $|\alpha_{n,\sigma}\rangle$ and $|\beta_{n,\sigma}\rangle$, via canonical transformation for each molecular site,

$$\begin{aligned} |\alpha_{n,\sigma}\rangle &= \cos(\theta_n)|c_{n,\sigma}\rangle + \sin(\theta_n)|d_{n,\sigma}\rangle \\ |\beta_{n,\sigma}\rangle &= -\sin(\theta_n)|c_{n,\sigma}\rangle + \cos(\theta_n)|d_{n,\sigma}\rangle, \end{aligned} \quad (5)$$

with $\theta_n = \frac{1}{2}\tan^{-1}(\frac{V}{\epsilon_{s,n}})$ and $\epsilon_{s,n} = \frac{1}{2}(V(n) + \epsilon_0 - E_p)$. Consequently, the total Hamiltonian becomes

$$H = H_0 + H_t, \quad (6)$$

where

$$\begin{aligned} H_0 = &\sum_{n,\sigma} (\epsilon_0 \cos^2(\theta_n) + E_p \sin^2(\theta_n) \\ &+ V\sin(2\theta_n))|\alpha_{n,\sigma}\rangle\langle\alpha_{n,\sigma}| \\ &+ \sum_{n,\sigma} (\epsilon_0 \cos^2(\theta_n) + E_p \sin^2(\theta_n) \\ &- V\sin(2\theta_n))|\beta_{n,\sigma}\rangle\langle\beta_{n,\sigma}| \\ = &\sum_{n,\sigma} E^{\alpha}_{n,\sigma}|\alpha_{n,\sigma}\rangle\langle\alpha_{n,\sigma}| + \sum_{n,\sigma} E^{\beta}_{n,\sigma}|\beta_{n,\sigma}\rangle\langle\beta_{n,\sigma}| \end{aligned}$$

and

$$\begin{aligned} H_t = &\sum_{n\sigma} -t_{n,n+1}\cos^2(\theta_n)(|\alpha_{n+1,\sigma}\rangle\langle\alpha_{n,\sigma}| + h.c.) \\ &-t_{n,n+1}\sin^2(\theta_n)(|\beta_{n+1,\sigma}\rangle\langle\beta_{n,\sigma}| + h.c.) \\ &+\sum_{n\sigma} \frac{t_{n,n+1}}{2}\sin(2\theta_n)(|\alpha_{n+1,\sigma}\rangle\langle\beta_{n,\sigma}| + h.c.) \\ &+\frac{t_{n,n+1}}{2}\sin(2\theta_n)(|\beta_{n+1,\sigma}\rangle\langle\alpha_{n,\sigma}| + h.c.). \end{aligned} \quad (7)$$

The E^{α}_n and E^{β}_n in H_0 are the hybridized energy levels at the nth molecular site.

With equation (6), the ground state eigenvalues and eigenfunctions are obtained by solving the Schrödinger equation, $H|\psi_{\mu,\sigma}\rangle = E|\psi_{\mu,\sigma}\rangle$. The ground state energy E_G is obtained by operating the Hamiltonian to the μth eigenstate $|\psi_{\mu,\sigma}\rangle$. Through Wannier expansion, each eigenfunction is constructed by the linear combination of new bases set, $|\psi_{\mu,\sigma}\rangle = \sum_n (Z^{\alpha}_{\mu,n,\sigma}|\alpha_{n,\sigma}\rangle + Z^{\beta}_{\mu,n,\sigma}|\beta_{n,\sigma}\rangle)$, with expansion coefficients $Z^{\alpha}_{\mu,n,\sigma}$ and $Z^{\beta}_{\mu,n,\sigma}$, obtained from the numerical calculation. The ground state energy, $E_G = \sum_{\mu}\langle\psi_{\mu}|H|\psi_{\mu}\rangle$, is then expressed as

$$\begin{aligned} E_G = &\frac{K_s}{2}\sum_n (u_{n+1} - u_n + c)^2 \\ &+ \sum_{\mu,n,\sigma}^{occ} (E^{\alpha}_{n,\sigma} Z^{\alpha*}_{\mu,n,\sigma} Z^{\alpha}_{\mu,n,\sigma} + E^{\beta}_{n,\sigma} Z^{\beta*}_{\mu,n,\sigma} Z^{\beta}_{\mu,n,\sigma}) \\ &\times(-t_{n,n+1}\cos^2(\theta_n) Z^{\alpha*}_{\mu,n+1,\sigma} Z^{\alpha}_{\mu,n,\sigma} + h.c.) \\ &+(-t_{n,n+1}\cos^2(\theta_n) Z^{\beta*}_{\mu,n+1,\sigma} Z^{\beta}_{\mu,n,\sigma} + h.c.) \\ &+\left(\frac{t_{n,n+1}}{2}\sin(2\theta_n) Z^{\alpha*}_{\mu,n+1,\sigma} Z^{\beta}_{\mu,n,\sigma} + h.c.\right) \\ &+\left(\frac{t_{n,n+1}}{2}\sin(2\theta_n) Z^{\beta*}_{\mu,n+1,\sigma} Z^{\alpha}_{\mu,n,\sigma} + h.c.\right), \end{aligned} \quad (8)$$

with the summation of eigenstates, μ, counts only from the lowest to the highest occupied states. Actually, we can relax this restriction for nonzero temperatures by incorporating the Fermi-Dirac distribution function $f(\mu - \mu_F)$ to the expansion coefficients $Z^{\alpha}_{\mu,n,\sigma}$ and $Z^{\beta}_{\mu,n,\sigma}$ and take into account of all the states. The chemical potential, μ_F, in the Fermi-Dirac function $f(\mu - \mu_F) = (e^{(\mu-\mu_F)/k_BT} + 1)^{-1}$

$$u_{n+1}-u_n=\frac{eE}{K_s}\sum_{\mu}^{occ}Z^{\alpha*}_{\mu,m}Z^{\alpha}_{\mu,m}\cos^2(\theta_n)+Z^{\beta*}_{\mu,m}Z^{\beta}_{\mu,m}\sin^2(\theta_n)-\frac{2\alpha}{K_s}\sum_{\mu}^{occ}(Z^{\alpha*}_{\mu,n+1}Z^{\alpha}_{\mu,n}+Z^{\alpha*}_{\mu,n}Z^{\alpha}_{\mu,n+1})\cos(\theta_n)\cos(\theta_{n+1})$$
$$-\frac{2\alpha}{K_s}\sum_{\mu}^{occ}(Z^{\beta*}_{\mu,n+1}Z^{\beta}_{\mu,n}+Z^{\beta*}_{\mu,n}Z^{\beta}_{\mu,n+1})\sin(\theta_n)\sin(\theta_{n+1})+\frac{2\alpha}{K_s}\sum_{\mu}^{occ}(Z^{\alpha*}_{\mu,n+1}Z^{\beta}_{\mu,n}+Z^{\beta*}_{\mu,n}Z^{\alpha}_{\mu,n+1})\sin(\theta_n)\cos(\theta_{n+1})$$
$$+\frac{2\alpha}{K_s}\sum_{\mu}^{occ}(Z^{\beta*}_{\mu,n+1}Z^{\alpha}_{\mu,n}+Z^{\alpha*}_{\mu,n}Z^{\beta}_{\mu,n+1})\sin(\theta_{n+1})\cos(\theta_n)-C, \tag{10}$$

$$C=\frac{2eE}{K_s(N-1)}\sum_{n=1}^{N-1}\sum_{\mu}^{occ}(Z^{\alpha*}_{\mu,m}Z^{\alpha}_{\mu,m}\cos^2(\theta_n)+Z^{\beta*}_{\mu,m}Z^{\beta}_{\mu,m}\sin^2(\theta_n))+\frac{2\alpha}{K_s(N-1)}\sum_{n=1}^{N-1}\sum_{\mu}^{occ}(Z^{\alpha*}_{\mu,n+1}Z^{\beta}_{\mu,n}\cos(\theta_{n+1})\sin(\theta_n)+h.c.)$$
$$+\frac{2\alpha}{K_s(N-1)}\sum_{n=1}^{N-1}\sum_{\mu}^{occ}(Z^{\beta*}_{\mu,n+1}Z^{\alpha}_{\mu,n}\sin(\theta_{n+1})\cos(\theta_n)+h.c.)-\frac{2\alpha}{K_s(N-1)}\sum_{n=1}^{N-1}\sum_{\mu}^{occ}(Z^{\alpha*}_{\mu,n+1}Z^{\alpha}_{\mu,n}\cos(\theta_n)\cos(\theta_{n+1})+h.c.)$$
$$-\frac{2\alpha}{K_s(N-1)}\sum_{n=1}^{N-1}\sum_{\mu}^{occ}(Z^{\beta*}_{\mu,n+1}Z^{\beta}_{\mu,n}\sin(\theta_n)\sin(\theta_{n+1})+h.c.) \tag{11}$$

is determined from the conservation of the total carriers, $2N$,

$$2N=\sum_{\mu,n,\sigma}f(\mu-\mu_F)|Z^{\alpha}_{\mu,n,\sigma}|^2+f(\mu-\mu_F)|Z^{\beta}_{\mu,n,\sigma}|^2. \tag{9}$$

In the ground state, the offset of the nth molecule's equilibrium position, u_n, is determined by the energy minimum, $\frac{\partial E_G(u_n)}{\partial u_n}=0$, from which the offset equation is obtained as

see equation (10) above

where the constant C is given by

see equation (11) above.

The average amount of charge transfer Δ_n from the ENV to the OSC is obtained from the difference of carrier occupation numbers between the α and the β states, with

$$\Delta_n=n_c-n_d$$
$$=\frac{1}{2N}\sum_{n=1}^{N}\sum_{\mu}^{occ}(\cos^2(\theta_n)-\sin^2(\theta_n))(|Z^{\alpha}_{\mu,n}|^2-|Z^{\beta}_{\mu,n}|^2), \tag{12}$$

where n_c and n_d are the average electron number in the orbits of the OSC and the ENV, respectively. When Δ_n is positive the OSC serves as a charge acceptor, or as a charge donor if Δ_n is negative.

We propose the length of OSC is limited to adopt Keldysh non-equilibrium Green's function formulation for a nano-scale system, the current formula in the OSC is calculated as,

$$I=\frac{e}{h}\int d\epsilon[f_L(\epsilon+v_a)-f_R(\epsilon)]\mathrm{T_r}\{G^a(\epsilon)\Gamma^R(\epsilon)G^r(\epsilon)\Gamma^L(\epsilon)\}, \tag{13}$$

where $f_{L(R)}$ is the Fermi-Dirac distribution function for the left (right) lead; $\Gamma^{L(R)}(\epsilon)=2\pi V^2_{L(R)}D_{L(R)}(\epsilon)$ is the broadening function that comes from the coupling $V_{L(R)}$ between the leftmost (rightmost) OSC molecule and the lead, and $D_{L(R)}(\epsilon)$ is the density of states (DOS) of the left (right) lead; function of $G^{r(a)}(\epsilon)$ is the retarded (advanced) Green's function that is derived from the Hamiltonian given by equation (6). The self-energies come from the lead interactions are evaluated from these Green's functions,

$$\Sigma_{\alpha\in L,R}(\epsilon)=\sum_{k,\eta\to 0}\frac{V^2_{\alpha}}{\epsilon-\epsilon_k+i\eta}, \tag{14}$$

where ϵ_k is the carrier kinetic energy in the lead. If the bandwidth of the lead is so large then, respectively, the self-energy and the DOS can be approximated by $\Sigma_{\alpha\in L,R}(\epsilon)=-i\pi V^2_{\alpha}D_{\alpha}(\epsilon)$ and $D_{\alpha}(\epsilon)=\frac{2}{W}$, where W is the bandwidth of the lead.

All the energy parameters in this paper are scaled in the unit of eV, the unit of the e-ph coupling constant α is in eV/Å, and the spring constant K_s is in eV/Å^2. The hopping integral of the OSC, $t_0=2.5$ and $t_e=0.1$, and the number of molecular sites in the OSC is set as $N=50$ in the nano-scale region. The temperature is set to 300 K.

3 Results and discussion

Our results realize the CT process that takes place between the coupled orbits of the OSC and the ENV via orbital hybridization. It can be readily understood that charges will flow from the ENV to the OSC as the ENV orbital energy level is higher than that of the OSC, making the so-called acceptor-OSC. Reversely, we will have a so-called donor-OSC with a higher OSC orbital energy level. The charge flow rate increases with larger orbital energy level differences. Figure 1 shows the amount of CT, Δ_n, as a function of the coupling constant V for various ENV

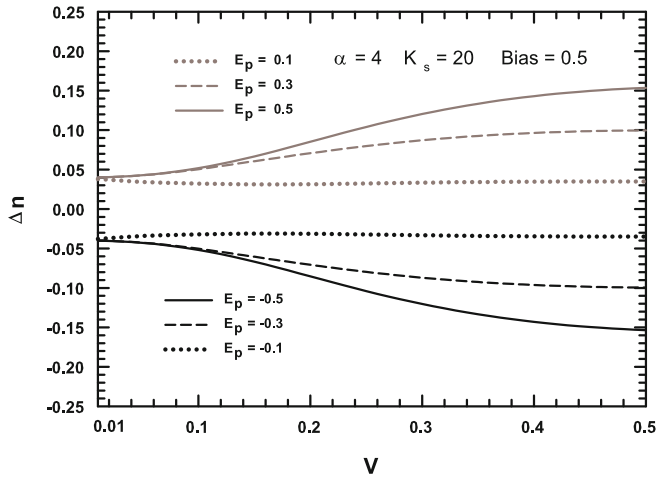

Fig. 1. The amount of transferred charge Δ_n as a function of V for various orbital energy level of the ENV E_p. The spring constant and electron-phonon coupling constant are $K_s = 20$ and $\alpha = 4$, respectively.

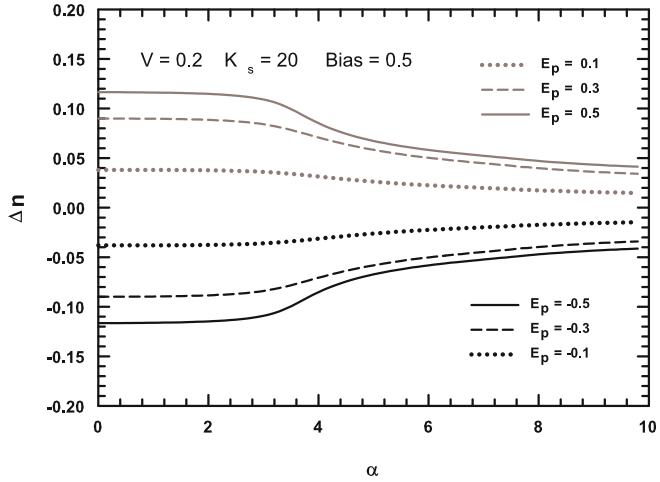

Fig. 2. The amount of transferred charge Δ_n as a function of electron-phonon coupling constant α for various orbital energy level of ENV E_p, at $V = 0.2$ and the spring constant $K_s = 20$.

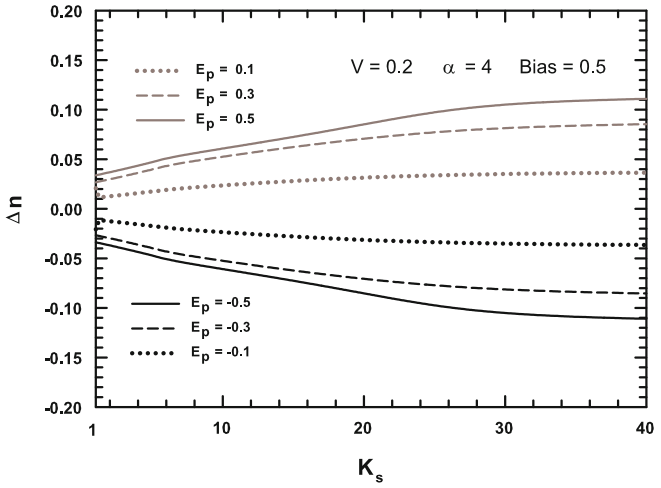

Fig. 3. The amount of transferred charge Δ_n as a function of the spring constant K_s for various orbital energy level of ENV E_p, at $V = 0.2$ and the electron-phonon coupling constant $\alpha = 4$.

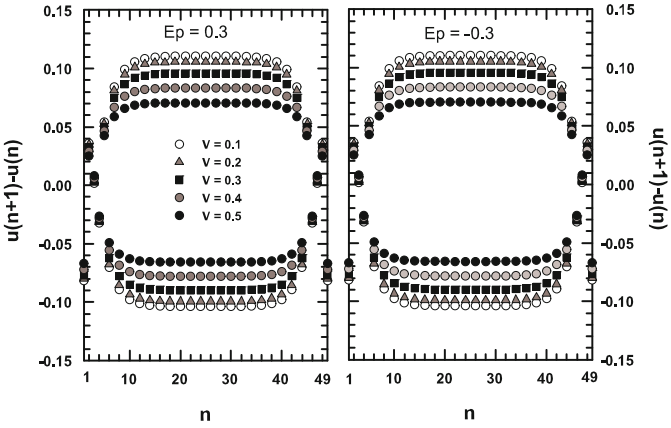

Fig. 4. The difference of atomic equilibrium position offset between two nearest neighbor sites, $u_{n+1} - u_n$, for various V at atomic site n. The left and right figures correspond to acceptor-OSC and donor-OSC, respectively. Here the displacement of the first site is set to zero.

energy level E_p relative to OSC energy level ϵ_0, which is chosen as the energy reference and set to be zero. It can be seen that Δ_n increases with V and is symmetric between donor- ($E_p > 0$) and acceptor-OSC ($E_p < 0$). In addition, greater energy difference between the OSC and the ENV energy levels causes larger Δ_n. It is well known that there are strong electron-phonon coupling in OSC, which is manifested by the existence of polarons in the system. Figure 2 shows Δ_n as a function of electron-phonon coupling constant α. The results clearly illustrate that CT is suppressed by the electron-phonon interactions and the effect is more obvious at larger α values. It can be understood by the fact that carriers are more seriously trapped by phonons for stronger electron-phonon interactions. Although the energy levels in OSC will be lowered from the polaron binding energy, which has been investigated for justifying the CT should be increasing [24].

Actually, in this ENV coupled system the energy level of ENV is also modified from the e-ph coupling by the orbital hybridization. Besides, our model implicitly involving the reduced hopping integral from the e-ph interaction, which completely reflects the bandwidth reduction, is different from the one modifying the orbital energy levels in the reference [24]. The spring constant K_s in equation (2) is related to the mechanical property of OSC. Higher K_s corresponds to a more rigid OSC. It can be seen in Figure 3 that Δ_n increases with increasing K_s, which implies it is easier to have CT in rigid OSCs.

It is known that a OSC with a half filled energy band transforms from a conductor into an insulator through the dimerization process resulted from the atomic displacements induced by electron-phonon interactions [25]. The dimerization process drives the molecules in the wire into pairs and consequently doubles the original lattice periodicity. Our results displayed in Figure 4 clearly show

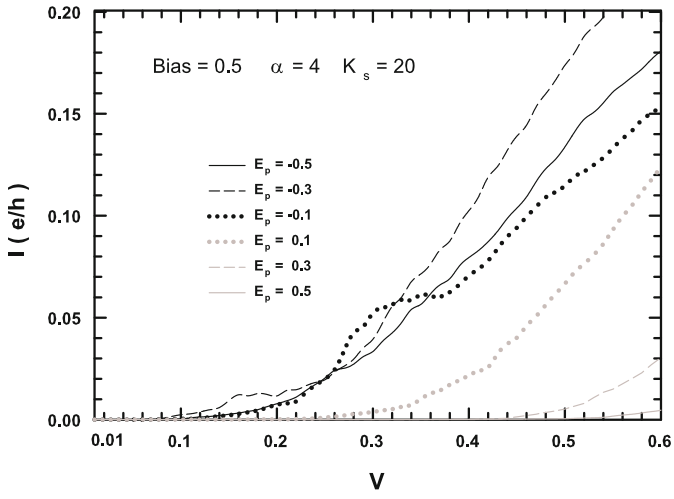

Fig. 5. Current in the OSC as a function of the orbital coupling constant V for various orbital energy level of ENV, E_p, at the applied bias, $V_a = 0.5\ V$, e-ph coupling $\alpha = 4$, and the spring constant $K_s = 20$.

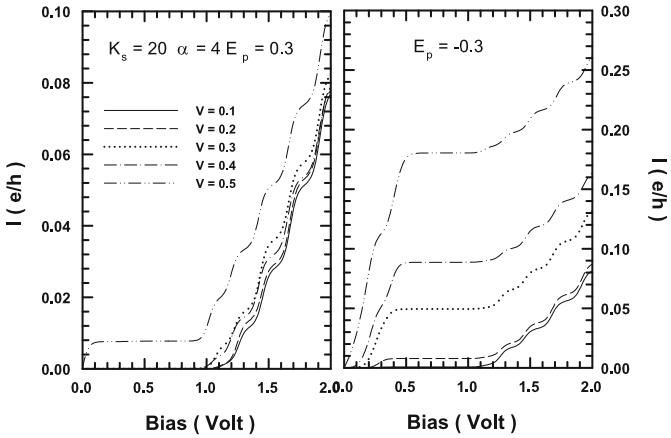

Fig. 6. Current in the OSC as a function of bias for various orbital coupling constant V at e-ph coupling $\alpha = 4$ and spring constant $K_s = 20$. The left and right figures correspond to acceptor-OSC and donor-OSC at $E_p = 0.3$ and $E_p = -0.3$, respectively.

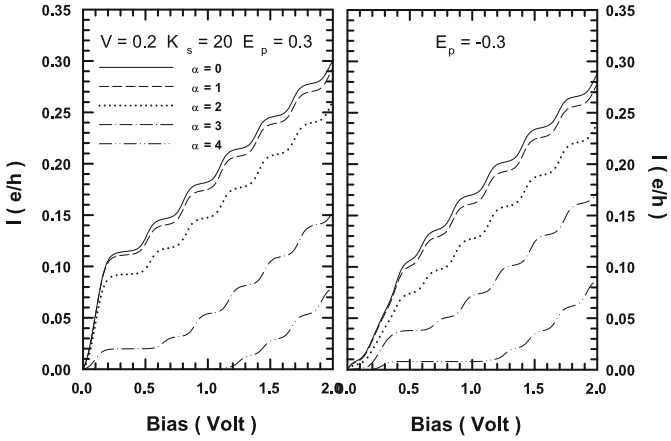

Fig. 7. Current in the OSC as a function of bias for various electron-phonon coupling constant α with $V = 0.2$ and spring constant $K_s = 20$. The left and right figures correspond to acceptor-OSC and donor-OSC at $E_p = 0.3$ and $E_p = -0.3$, respectively.

that the dimerization decreases with increasing orbital coupling V. With the reference to Figures 1 and 2, in which CT increases with V and decreases with α, respectively, implying the suppressed electron-phonon interactions caused by stronger orbital couplings of the ENV is accompanied by an enhanced CT.

The aforementioned results indicate that stronger orbital hybridization V enhances the conductivity of OSC. Such indication is confirmed by the results shown in Figure 5. Another important feature can be seen in Figure 5 is that donor-OSCs are more conductive than acceptor-OSCs, which implies that choosing chemical dopants with slightly lower energy level relative to that of OSC increases the conduction of OSC. The difference in the conductivity for the two types of OSC comes from the lowered chemical potential of the left lead caused by the applied bias is closer to the highest occupied state of the donor-OSC than that of the acceptor-OSC. Conduction variation in the acceptor- and the donor OSCs corresponds to $E_p = 0.3$ and $E_p = -0.3$, respectively, are shown in Figure 6 by the currents as a function of applied bias. The result that acceptor-OSC is less conductive than donor-OSC can be accounted for by the result that the conductivity of acceptor-OSC does not increase monotonically with increasing V. Such tendency implies that the current variation is a result of nontrivial entangling between E_p and V, which in turn is due to the difference between the chemical potential of the left lead and the LUMO does not change monotonically with V.

The magnitude of coupling constant α in equation (2) represents the interaction strength of electron-phonon interaction. The current suppression in OSC by the electron-phonon interaction is shown in Figure 7. The result that the current suppression in acceptor-OSC is more serious than in donor-OSC is due to that there are more phonon-dragged carriers in the acceptor-OSC as a result of an effective increase of e-ph interaction. We confirm this assumption from the investigation of the energy level diagram in both types of OSC. In the diagram of the energy levels relative to the chemical potential, μ_F is shown in Figure 8, which clearly reveals two evidences: first, the μ_F distinctly lies on HOMO and LUMO for donor-OSC and acceptor-OSC, respectively, which is consistent with the CT direction as-defined before; second, the energy levels are leaving HOMO and LUMO with the increase of e-ph interaction, which also consistently proves the fact that the current decreases with the e-ph interaction. Furthermore, if we observe the diagram more carefully, the acceptor-OSC deserves more effective e-ph interaction as we assumed, namely, at the same e-ph coupling, α, the energy levels leave farther away HOMO and LUMO. The spring constant K_s appears in equation (2) is related to the mechanical properties of OSC, i.e. the stiffness of materials. Relatively large K_s implies that OSC has a

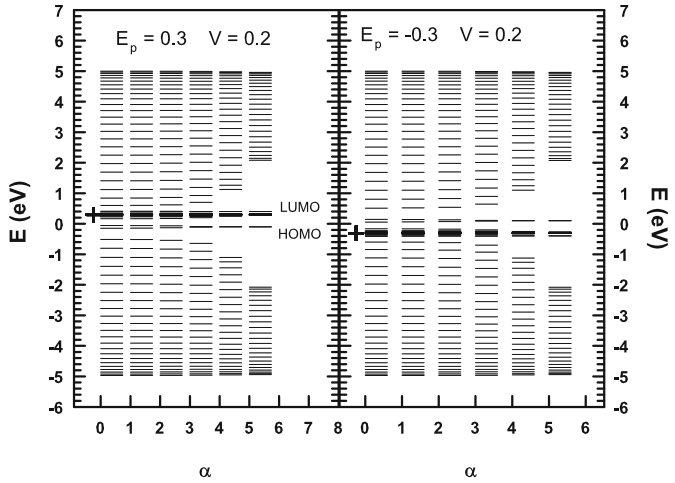

Fig. 8. The energy diagram for six e-ph coupling α from 0 to 5 integrals at $V = 0.2$ and $K_s = 20$. The left and right figures correspond to acceptor-OSC and donor-OSC at $E_p = 0.3$ and $E_p = -0.3$, respectively. The position of the crisscross is the chemical potential, μ_F, calculated from equation (9) and the two energy levels in central region are LUMO and HOMO, respectively.

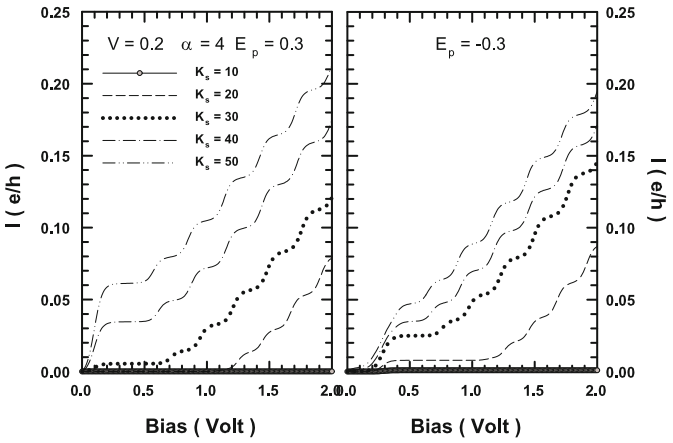

Fig. 9. Current as a function of bias for various spring constant K_s at $V = 0.2$ and electron-phonon coupling constant $\alpha = 4$. The left and right figures correspond to the acceptor-OSC and the donor-OSC at $E_p = 0.3$ and $E_p = -0.3$, respectively.

stronger bonding that produce a more rigid material. Figure 9 shows the conduction increases with increasing K_s for acceptor-OSC as well as donor-OSC. This is owing to the increase of conduction carriers accompanying with increasing K_s in both types of OSC via increasing CT as shown in Figure 3. The increasing rate of conduction with respect to K_s in donor-OSC is larger than that in acceptor-OSC is similarly owing to that electron-phonon interaction is more effective in acceptor-OSC as described by Figure 7.

4 Summary

We propose a microscopic theory to study the conduction variation in an environment-coupled organic semiconductor. Our model provides a charge transfer mechanism based on orbital hybridization between orbits of the organic semiconductor and the environment. The charge transfer process is determined by the orbital energy level difference between the environment and the organic semiconductor. As a result of charge transfer, an acceptor- or donor-organic semiconductor is formed depending on whether the orbital energy of the environment is higher or lower than that of the organic semiconductor. Our results show that the orbital hybridization coupling and the stiffness of the organic semiconductors are favorable factors for charge transfer between the environment and the organic semiconductor, while electron-phonon interaction is not. The conduction of organic semiconductors is affected in a similar way; the conductivity increases with stronger orbital hybridization interaction but is lowered by stronger electron-phonon couplings. The conduction in acceptor-organic semiconductors is found to be larger than that of donor-organic semiconductors. This is a result that larger number of phonon-dressed carrier correspond to a stronger electron-phonon interaction.

This work is supported by the National Science Council in Taiwan through Grant Nos. NSC-98-2112-M-390-001-MY3 (Shih-Jye Sun) and NSC-98-2112-M-005-004-MY3 (Chung-Yi Lin), and by the National Chung Hsing University. The hospitality of the National Center for Theoretical Sciences, Taiwan, where the work was initiated, is gratefully acknowledged.

References

1. R.H. Friend, R.W. Gymer, A.B. Holmes, J.H. Burroughes, R.N. Marks, C. Taliani, D.D.C. Bradley, D.A. Dos Santos, J.L. Brédas, M. Lögdlund, W.R. Salaneck, Nature **397**, 121 (1999)
2. C. Dimitrakopoulos, P.R.L. Malenfant, Adv. Mater. **14**, 99 (2002)
3. C.J. Brabec, N.S. Sariciftci, J.C. Hummelen, Adv. Funct. Mater. **11**, 15 (2001)
4. V. Coropceanu, J. Cornil, D.A. da Silva Filho, Y. Olivier, R. Silbey, J.-L. Bredas, Chem. Rev. **107**, 926 (2007)
5. N. Karl, Synth. Met. **133-134**, 649 (2003)
6. D.L. Cheung, A. Troisi, Phys. Chem. Chem. Phys. **10**, 5941 (2008)
7. Y. Shen, K. Diest, M.H. Wong, B.R. Hsieh, D.H. Dunlap, G.G. Malliaras, Phys. Rev. B **68**, R081204 (2003)
8. C.K. Lu, H.F. Meng, Phys. Rev. B **75**, 235206 (2007)
9. D.A. Bernards, R.M. Owens, G.G. Malliaras, *Organic Semiconductors in Sensor Applications* (Springer Series in Materials Science, 2008), Vol. 107
10. Z.T. Zhu, J.T. Mason, R. Dieckmann, G.G. Malliaras, Appl. Phys. Lett. **81**, 4643 (2002)
11. A.M. Andringaa, M.J. Spijkmana, E.C.P. Smitsc, S.G.J. Mathijssenb, P.A. van Halb, S. Setayeshb, N.P. Willardb, O.V. Borshcheve, S.A. Ponomarenkoe, P.W.M. Bloma, D.M. de Leeuwa, Org. Electr. **11**, 895 (2010)
12. H. Peisert, M. Knupfer, F. Zhang, A. Petr, L. Dunsch, J. Fink, Appl. Phys. Lett. **83**, 3930 (2003)

13. R. Dietmueller, A.R. Stegner, R. Lechner, S. Niesar, R.N. Pereira, M.S. Brandt, A. Ebbers, M. Trocha, H. Wiggers, M. Stutzmann, Appl. Phys. Lett. **94**, 113301 (2009)
14. J.H. Burroughes, D.D.C. Bradley, A.R. Brown, R.N. Marks, K. Mackay, R.H. Friend, P.L. Burns, A.B. Holmes, Nature **347**, 539 (1990)
15. O.L.A. Monti, M.P. Steele, Phys. Chem. Chem. Phys. **12**, 12390 (2010)
16. I.G. Hill, A. Kahn, J. Appl. Phys. **84**, 5583 (1998)
17. G.M. Rangger, O.T. Hofmann, L. Romaner, G. Heimel, B. Bröker, R. Blum, R.L. Johnson, N. Koch, E. Zojer, Phys. Rev. B **79**, 165306 (2009)
18. M. Muntwiler, Q. Yang, W.A. Tisdale, X.-Y. Zhu, Phys. Rev. Lett. **101**, 196403 (2008)
19. R.C. Hatch, C.W. Sanchez, H. Höchst, Appl. Phys. Lett. **97**, 093303 (2010)
20. F. Silvestri, A. Marrocchi, Int. J. Mol. Sci. **11**, 1471 (2010)
21. W.P. Su, J.R. Schrieffer, A.J. Heeger, Phys. Rev. Lett. **42**, 1698 (1979)
22. W.P. Su, J.R. Schrieffer, A.J. Heeger, Phys. Rev. B **22**, 2099 (1980)
23. R.G. Endres, D.L. Cox, R.R.P. Singh, Rev. Mod. Phys. **76**, 195 (2004)
24. F. Ortmann, F. Bechstedt, K. Hannewald, Phys. Status Solidi B **248**, 511 (2011)
25. R. Peierls, *Quantum theory of solids* (Clarendon Press, Oxford, 1955), Vol. 108